Optical satellite data monitoring of synergistic effects of summer urban heat island and heat waves on viral infections dynamics

M. ZORAN, D. SAVASTRU*, M. N. TAUTAN
National Institute R&D for Optoelectronics, Magurele, MG5, 077125, Romania

The present study addresses the interaction effects of spatiotemporal dynamics of air pollutants and climate parameters, under urban heat island (UHI) amplified by heat wave (HW) on the incidence and lethality of COVID-19 viral infection in the test site Tokyo metropolis, capital of Japan. July-September periods of 2020, 2021, and 2022, were comparatively statistically analyzed based on time series of satellite MODIS Terra/Aqua Land Surface Temperature (LST) and total Aerosol Optical Depth at 550 nm (AOD) data, together with *in-situ* air pollutants and climate monitoring data. During persistent stable anticyclonic weather conditions of summer 2022, this research found high positive Spearman correlations between maximum air temperature at 2 m height (T_{max}) and the daily COVID-19 incidence (DNC)and lethality cases (DND), expressed by ~~DNC~~ ($r = 0.81$; $p \leq 0.05$) for DNC, and respectively ~~DND~~ ($r = 0.38$; $p \leq 0.05$) for DND, which together with positive correlations between LST and COVID-19 incidence DNC ($r = 0.39$; $p \leq 0.05$), and lethality DND ($r = 0.18$; $p \leq 0.05$), may explain the highest recorded rates of COVID-19 new cases and deaths, attributed to the increased urban heat and air pollution in Tokyo. Despite of intense ultraviolet solar radiation, which can obstruct viral intensity, and several restrictions and control policies, under summer high temperatures attributed to co-occurrence of HW and UHI, the daily new COVID-19 incidence cases increased in the summer of 2022 in Tokyo by 7.7 times than in the summer of 2021, and by 80.2 times than in the summer of 2020.

(Received June 24, 2025; accepted August 5, 2025)

Keywords: Time series MODIS terra/Aqua satellite data, Heat waves and urban heat island, Air pollution, Climate variables, Viral infection COVID-19

1. Introduction

Global climate change is one of the prime concerns in the contemporary world, mainly due to the increased urbanization, which is responsible for the urban heat island (UHI) effect, where the temperature of the city core is warmer than its rural surroundings, affecting inhabitants' lives. Satellite remote sensing optical data has proved to be a valuable tool for studying the phenomenon, its physics, and its correlations with summer heat waves (HW), and the potential role of urban thermal environment in the transmission of viral pathogens during pandemic events, often interacting climate variables that determine the survival rate of these viruses in air. Also, during recent years, there has been a growing use of satellite measurements in the field of urban air quality and public health assessments.

Despite the announced end of the emergency phase of COVID-19 in May 2023 by the World Health Organization, according to U.S. CDC Centres for Disease Control and Prevention, COVID-19 disease produced by SARS-CoV-2 pathogens continues till now (June 2025) to spread with new subvariants [1]. The ongoing global COVID-19 pandemic, declared in early March 2020, spanning more than five years and several seasons, attests the significant effects of the climate and environmental factors in the viral infection airborne diffusion route, mostly in agglomerated urban areas. The understanding of the environmental factors in the pathogenesis of viral infections is reaching high significance in the context of climate change. In the summer of 2022, Japan and its metropolis Tokyo, selected as a study case, faced the most severe heat wave in 150 years and the worst COVID-19 pandemic wave, when the mean temperature was 0.91 °C warmer than normal, with several consecutive days above 35 °C [2]. The heat wave of summer 2022 in Japan began on 28 June and lasted until 25 August, and was the hottest heat wave in Japanese history since records began in 1875. This extreme climate event was attributed to the synergy of climate change and La Niña conditions, with a high-pressure system of June 2022 over the Pacific Ocean, resulting in a south-to-south-westerly flow of air which transported hotter air from the tropics to Japan, and fueled higher temperatures. Tokyo metropolitan area, located in the eastern part of Japan experienced record-breaking temperatures attributed to the co-occurrence of HW and UHIs phenomena. UHI phenomena observed in the Tokyo metropolis, are mainly attributed to wind flow blocked by too many tall buildings (more than 167 skyscrapers taller than 150 meters, many more than 550 buildings over 100 meters, and more under construction), and the materials in buildings which could increase the air temperature [3]. Some large-scale circulation anomalies connected to heat waves and typhoons are recorded every year. In the mega-city of Tokyo, the accelerated rate of HWs under UHIs increased

from 2003 to 2020 [4]. As a consequence, during COVID-19 viral infection were exacerbated the challenges faced by urban residents' health. Consequently, an accurate assessment of summer urban heat described through UHI and HW intensity, and a better understanding of driving factors have become imperative issues to be used by public health decision-makers, to urgently develop prevention and mitigation strategies for periods of infectious diseases under HWs.

While due to large spatial heterogeneity and the lack of dense weather station networks, meteorological data cannot be effectively used to measure the UHI effect, remote sensing offers a useful way to track, measure, and manage the UHI effect [5,6]. Remote sensing technologies, which provide the derived environmental variables, have already been used in different epidemiologic studies [7,8], but so far only rarely in the context of viral pandemic diseases. In recent decades, satellite remote sensing platforms deliver products with high spatial and temporal resolutions, among which global land surface temperature (LST) observations in the thermal infrared, with spatial resolutions of less than 2 km. MODIS Terra/Aqua long-term operational satellites have provided valuable LST data (MOD11) for over two decades. Recently, the Sentinel-3 mission has provided new large-scale satellite LST products for global land and sea surface temperatures using three thermal infrared bands. Multi-spatial and multi-temporal remote sensing data have been widely used to monitor and analyze the dynamics of UHIs and HWs [9-11]. Satellite remote sensing approaches and MODIS Terra/Aqua time series data are suitable for the assessment of Land surface temperature (LST) parameters and UHI phenomenon, suggesting that thermal characteristics and landscape associated with thermal patterns are dependent on urban composition, and its configuration of land cover [12-14]. Several studies exploring worldwide cities found interesting results regarding the urban thermal environment and its relation with urban morphology and land cover [15,16]. However, the existing studies on the urban heat island (UHI) and heat wave (HW) effects on the urban thermal environment have primarily focused on their temporal space distribution characteristics [6,7,17,18], with less focus on the influences of other environmental factors, particularly during pandemic events.

This study explores the synergism between urban heat island (UHI) phenomena under summer heat waves (HWs), and poor urban air quality together with climate conditions on the fast transmission of COVID-19 disease during 2020-2022 with a focus on the summer periods of 2020, 2021, 2022 years in the Tokyo metropolis. To address these research gaps the crucial role of the main air pollutants was examined (particulate matter in two size fractions 2.5 μm -PM2.5, and 10 μm -PM10, ground-level ozone- O_3 and nitrogen dioxide- NO_2), associated with related-climate variables responsible for urban heat stress), which may amplify the SARS-CoV-2 viral pathogens' impact on the human cardiorespiratory system, and the COVID-19 disease spatiotemporal dynamics pattern. Through applied statistical and time series analyses of the daily observational monitoring and satellite data acquired during three summer seasons over the investigated period, this study provides an accurate assessment of the linkage between urban air quality related to climate factors variability (daily mean-T and maximum air temperature - T_{max} at 2 m height, air relative humidity-RH, wind speed intensity-w, global horizontal solar surface irradiance-GHI, planetary boundary layer-PBL height, and land surface temperature-LST) and epidemiologic evolution of the daily new COVID-19 cases-DNC and the daily new COVID-19 deaths-DND in Tokyo metropolis. The optical parameter total aerosol optical depth (AOD) at 550 nm, which expresses the sunlight attenuation by the column of aerosols, was selected to characterize the aerosol loading in the lower atmosphere over Tokyo. To highlight the impact of heat stress on viral infection transmission and lethality, this study compared the main air pollutant concentrations and climate parameters variability during the summer pandemic periods of 2020-2022. As Tokyo is among the most diverse, populated, dense, and transit-based cities in the world, it is an ideal test site for the study of extreme urban heat impact on viral disease transmission.

2. Materials and methods

2.1. Urban thermal environment

As mesoscale phenomena, which transport warm air from the upper atmosphere to the lower atmosphere, HWs influence the urban environment, its infrastructure, and human health [19,20]. Heat waves refer to positive anomalies or extremes above the daily mean air temperature, which can be recorded during several consecutive days (from days to weeks and even continue for months) in certain geographical contexts. Rapid urbanization is a crucial driver of landscape transformation with a significant impact on ecosystem resilience affecting the local climate and aggravating heat stress. The loss of vegetation plays a major role in altering land cover, which in turn influences carbon emissions and urban microclimates, such as the debut of the urban heat island (UHI) effect (urban/non-urban temperature differences), which may amplify the regional heat load during heat wave events. UHIs are classified into two classes: surface urban heat islands (SUHI), evaluated using land surface temperature (LST), and atmospheric urban heat islands, defined on air temperature at canopy level (CUHI) or at the urban boundary layer (UBL). However, SUHIs and CUHIs show similar dependencies on local climate and urban morphology, exhibiting a positive correlation and comparable trends [21]. The UHI intensity depends on the land surface energy budget variables: temperature and emissivity, land surface albedo, surface downward insolation, sensible and latent heat fluxes, longwave downward radiation, and ground heat flux. Complex interaction processes of shortwave and longwave radiation with aerosols, moisture, and other gaseous pollutants in

highly urbanized regions have a strong impact on UHI intensity [22,23]. In the current context of global climate warming due to increased urbanization and the COVID-19 pandemic challenge worldwide, hot summer temperatures and poor air quality become a significant concern for human health in densely metropolitan areas. During the last decades, global air temperature, and pollution have risen significantly, exacerbating intrinsic impacts on human health through affecting the immune system. [24-26]. Extreme urban heat attributed to the synergy of the UHI phenomenon and heat wave (HW) events is a progressively presenting issue, especially in several metropolitan regions of the world regarding occurrence, intensity, and duration. Exposure to extreme heat particularly in large urban settings can lead to a high range of effects at different levels: on health (heat-related illnesses in people with pre-existing medical conditions); economic needs for increasing power supply and concentration of heat-emitting sources; and the natural environment by damaging vegetation growth. UHIs and within-city micro-heat islands can amplify the effects of heat waves and increase the risk of advancing heat-related illnesses (like dehydration, heat exhaustion, and hyperthermia), significantly during pandemic events [27]. Some of these effects can be exacerbated in a densely urban region affected by low vegetation land cover, and the prevalence of impervious low-reflectivity surfaces, which increase UHI effects [28,29]. Urban extreme heat recorded in recent years is a significant issue that has gained great interest in the scientific world, especially concerning air pollution and human health in different health-related studies [30,31]. Several epidemiological studies have demonstrated the adverse health effects of short-term and long-term exposure to poor ambient air quality, and high ambient temperature under heat waves on non-accidental mortality, as major environmental risk factors associated with increased cardiorespiratory mortality [32,33]. Also, some global-scale epidemiological studies revealed the increased risk of mortality from extremely high temperatures, and summertime heat associated with viral infections [34,35]. Excess mortality related to the SARS-CoV-2 virus associated with high temperature was shown to be increased during the COVID-19 pandemic in some urban areas [36,37]. As presently, climate change is leading to the increased frequency of heat waves as extreme summer climate events and associated increasing number of viral infectious diseases, is an urgent need to act for human health and life protection. Based on climate projections, some studies reported future increasing rates of heat-related illness worldwide [38-40], particularly in Japan due to an aging society [41-44]. Among these, the urban thermal environment, which is described by several atmospheric variables (such as surface solar irradiance, wind speed intensity and direction, and air humidity) has a great influence on the human thermal environment defined by human metabolic thermoregulation in combination with air temperature high impacted by summer heat waves [45-47].

Several atmospheric and biometeorological (thermo-physiological) variables have been proposed for the thermal environment analysis and its effects on human thermal comfort [48]. As a vital function of the human autonomic nervous system in response to heat stress, thermoregulation mechanisms are strongly influenced by exposure to extremely high temperatures during summer heat waves through the development of heat-related illnesses (general medical, neurological, and pharmacological). Some studies used daily maximum temperature to estimate the human body's reaction to urban heat stress, while other researchers considered apparent temperature, which combines meteorological variables: temperature, humidity, and wind speed [49,50].

This study uses daily maximum temperatures, having the advantage of accounting for local differences in Tokyo urban climatology.

2.2. Satellite remote sensing data used for urban thermal environment analysis

Satellite remote sensing technology, with its unique spatial coverage advantages and multitemporal, multisensor and multi spatial observation capabilities, has become an essential tool for urban thermal environment research. Different methodologies use time series satellite data to estimate the urban thermal environment and UHI phenomenon. Previous studies employed satellite data from Moderate Resolution Imaging Spectroradiometer (MODIS) Terra/Aqua, Sentinel-2, Sentinel-3, and Landsat 5, 7, and 8 to compare day/night climatic conditions in metropolitan areas and their suburbs to estimate the UHI intensity, and retrieve the land surface temperature (LST). Several biogeophysical and radiative parameters from different optical sensor observations provide corresponding parameter products, as well as can estimate UHI based on the temperature difference between urban and rural areas [51,52]. LSTs retrieved from the time series thermal infrared (TIR) satellite remote sensing bands with frequent coverage provide key indicators to estimate the UHI effect in high spatial and temporal resolution. Some limitations are related to adverse atmospheric conditions and long revisit satellite cycles, in the thermal environment.

Other studies used the synergy of microscale and mesoscale urban climate models to describe the diurnal UHI cycle and its spatiotemporal patterns, using satellite imagery datasets from MODIS Terra/Aqua, Landsat, and Sentinel-2. However, the latest MODIS Collection-5 LST data are used to evaluate the geographic variations of the diurnal and seasonal UHI phenomenon. By this, remote sensing has advanced urban thermal environment research through enabling spatiotemporal analysis and addressing methodological challenges and knowledge gaps. Present study used MODIS Terra/Aqua LST and AOD time series data.

Developed proper algorithms can be used to quickly retrieve surface radiative data sets, but for better accuracy need local calibration and validation. Mathematical algorithms generally incorporate all relevant physical processes and can be used globally, but their computational efficiency is often low. Use of efficient

algorithms developed to calculate urban land surface biogeophysical parameters by combining a clear-sky model and the parameterizations for cloud transmittances are also necessary [53]. In the developed algorithms, the transmittances for water vapor, ozone, Rayleigh, aerosol, and cloud are each handled across the whole VIS, NIR and IR spectral bands. In addition, the contribution of the multiple reflections between land surface ground and the atmosphere are also expressly considered. Based on the advanced algorithms applied to estimate instantaneous radiative parameters with inputs from MODIS products on board both Terra and Aqua platforms, time series satellite data can be used to efficiently analyze climate and urban land cover impacts on thermal environment [54,55].

Use of the advanced algorithms for time series satellite data analysis and statistical methods will make it possible to model the spatial dependencies between different land cover pixels, their temporal correlation, as well as the (possibly non-linear) relationships between multiple urban radiative and biogeophysical variables. The assumption of stationarity in these models means that the statistical model is valid for the entire target wavelength domain. This requirement is valid for all types of stochastic models, parametric as well as non-parametric. However, the variables that will be modeled are inherently non-stationary, meaning that their properties can have a spatiotemporal variability. Spatial non-stationarities are generated by satellite images, which may contain several types of landscapes or textural characteristics. Temporal non-stationarities include seasonal variability, described as a recurrence of patterns from year to year at a given location [56]. Another important source of temporal non-stationarity is the trends produced by climate change or low-frequency climatic events. New satellite generations, such as the Copernicus Sentinel 2/3/4/5 overcome this gap with higher spatial resolution.

2.3. Association of air pollution, atmospheric variables, and COVID-19

During the last decades, several epidemiologic studies conducted worldwide have shown that short- and long-term exposure to ambient air pollution with particulate matter and gaseous pollutants is related to numerous viral diseases, and the increased incidence of cardiorespiratory diseases, including heart attacks and stroke deaths, observed at lag 0-1 day. Some scientific studies found a positive association between outdoor particulate matter PM air pollution due to road traffic and industrial sources and COVID-19 morbidity and severity. Laboratory experiments proved a long-time viability of SARS-CoV-2 pathogens in both outdoor and indoor ambient aerosols or clusters of aerosols, as an important source of COVID-19 viral infection transmission [[57]. However, some scientific studies reported observed airborne microbial components of bioaerosols (bacterial, fungal, viral, dust mites, pollen, and cellular fragments) originating from diverse natural and anthropogenic sources, and their spatiotemporal patterns in the atmospheric planetary boundary layer, especially in urban areas [58]. The seasonal variability of bioaerosols was associated with changes in land surface air conditions at landscape interactions, local and regional climate conditions, and/or changes in global air circulation [59].

Pathogenic bioaerosols like as SARS-CoV-2 found in both outdoor as well as indoor environments are the main sources of viral infections through inhalation, ingestion, and direct contact acting on the human immune system [60]. They can suffer long-range cross-border transport in the atmosphere and persist for long-term periods [61, 62].

As some studies considered the projected increase of urban heat due to an increase in the duration, frequency, and severity of summer heatwaves and anthropogenic forcing, as well as the increase in the elderly population and rapid urbanization, people's exposure to poor urban air quality in synergy with heat stress will be a challenge during pandemic events. As aerosols warm up the atmosphere [63, 64], they tend to stabilize the air PBL heights right above the city with a strong effect on the depletion of energy efficiency dissipation from the surface to the atmosphere [65]. The amount of absorption and reflection depends on the urban morphology, like city canyons [66]. As a direct consequence, the availability of radiation at the surface level determines increasing of the ground-level ozone concentration, which is produced by the photooxidation of VOCs (volatile organic compounds) in the presence of nitrogen oxides-NOx. In urban agglomerated areas O_3 coexists with its higher concentration precursors in a complex photo-stationary equilibrium between photolysis and titration driven by sunlight and OH radicals [21]. Two air pollutants are particularly relevant during heat episodes: ozone and particulate matter PM in two size fractions PM2.5 and PM10 [67]. Outdoor areas record the highest concentrations of ground-level O_3, while indoor PM2.5 and PM10 can also penetrate. One possibility is that the effects of heat and air pollution are essentially equivalent to the effect of the two different exposures occurring separately (an additive effect). Also, air maximum temperature at 2 m height- T_{max} and concentrations of nitrogen dioxide -NO_2 are additional significant risk factors for heat stroke in urban areas [68]. Simultaneous exposure to air pollution and heat stress in urban agglomerated areas is an amplified harmful health effect. At the urban level, on days with high ground-level concentrations of air pollutants O_3, NO_2, PM2.5, and PM10, and UHI phenomena, under severe heat waves, significant negative effects on viral pandemic and non-pandemic cardiovascular diseases, especially among the elderly population, have been reported [28,44]. Viral human infections have been directly correlated to climate parameters like as ambient air relative humidity, air temperature, atmospheric pressure, wind speed intensity and direction, and precipitation rate [69]. Also, the association of respiratory viral infection with ambient air pollution and lower levels of planetary boundary layer height can have a major impact [70,71]. Currently, several studies consider that environmental factors and ground-level air pollution may play an essential role in the

diffusion and progression of the COVID-19 viral disease [72-76].

As a main optical property that quantifies the concentration of aerosols present in the atmosphere and a direct measure of aerosol loading, total aerosol optical depth (AOD) at 550 nm estimates the quantity of a beam's energy that is dispersed or absorbed in an atmospheric column over a studied area. It is the crucial variable in estimating the Earth's energy budget spatiotemporal variability. Changes in climate variables patterns could result in major changes in AOD, having direct and indirect impacts on aerosol radiative forcing. Due to variations in atmospheric dynamics and meteorology strong changes in AOD and tropospheric NO_2 have been recorded during and after COVID-19 [77,78]. The lowest part of the troposphere, the planetary boundary layer PBL is an interface for the exchange of energy and particulates between the land surface and the atmosphere, its development is strongly influenced by the complex vertical mixing process of aerosols, gases, and water vapor. A study in China observed that abnormally shallow PBL heights triggering strong aerosol-PBL interactions were associated with increased rates of COVID-19 incidence and lethality [79]. Several scientific papers found different results, but the widespread viral infection cases in warmer climate countries such as Iran, India, and Brazil have contradicted the existence of an inverse correlation of air temperature with COVID-19 cases [80]. In urban and industrialized regions, clusters of aerosols (particulate matter PM and pollutant gases) can attach viruses as well as bacteria and fungi, which can reach the upper and lower cardiorespiratory tract [81]. Function of climate conditions, both indoors and outdoors, contaminated air with viral pathogens will be transmitted [82].

2.4. Study test site

Tokyo megacity (Fig. 1), with 13,556 km^2 surface, and a population of more than 38 million, is located in the Southern coastal part of Honshu Island, and the Northern area of Tokyo Bay in Tokyo prefecture, at 35°41'23'' N Latitude, and 139◦41'32″ E Longitude. Tokyo City, the capital of Japan, with an area of 2,194 km^2 and a 40 m elevation, has more than 14 million people. The population density of Tokyo is around 6,225 people per km^2. The climate is humid subtropical, affected by the monsoon circulation, having hot, humid, and rainy summers, mild to cool winters, and occasional cold spells. The summer month August is the warmest with a 26.4 °C mean air temperature, while January is the coolest month, with a 5.2 °C mean air temperature [83]. The annual mean precipitation rate is about 1,530 mm; its levels being influenced by the mid-latitude storms and tropical cyclones. Figure 1 presents the locations of the urban/rural test sites used for UHI evaluation: Tokyo urban is a selected area of (6.5 km × 6.5 km) surface centered on 35.6764 °N latitude and 139.6500 °E longitude, and Tokyo rural is a selected area of (6.5 km × 6.5) km surface centered on 35.60 °N latitude and 139.25 °E longitude.

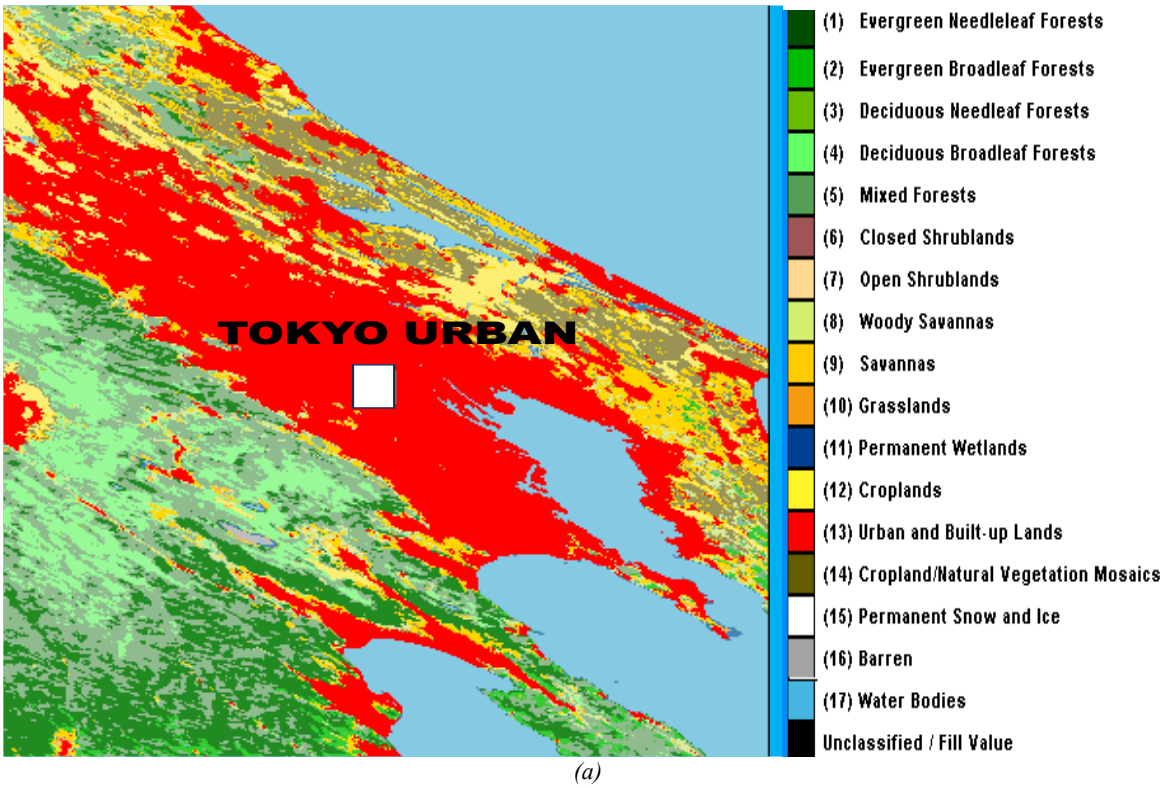

(a)

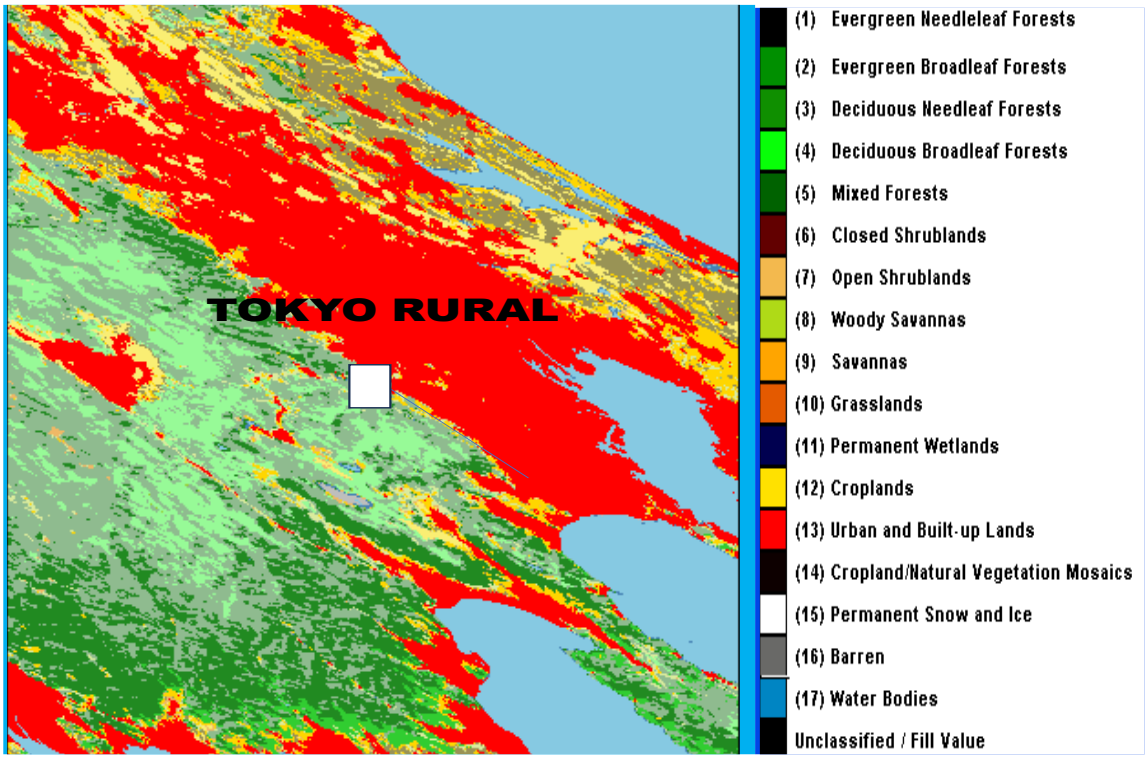

(b)

Fig. 1. Study test site Tokyo metropolitan area on a MODIS Terra classification map with the selected urban sector (a) and a representative rural vegetated area (b) used for UHI evaluation (colour online)

2.5. Data sets

To analyze the synergy impact of UHIs and HWs on COVID-19 viral infection incidence and lethality during the summer period 2020-2022, considering air pollutants and climate parameters variability in the Tokyo metropolitan area, this study used available observational, satellite remote sensing and reanalysis data provided by various sources. The main climate variables and air pollutants time series data sets were supplied by different monitoring networks and satellite platforms.

(1) COVID-19 data. Daily New COVID-19 cases (DNC) and Daily New COVID-19 death (DND) have been provided by COVID-19 available webpages for COVID-19 evidence in Tokyo [84, 85].

(2) MODIS LST data. Among the available LST products developed through the different retrieval algorithms based on TIR sensors from different satellite missions (TM/ETM+/OLI, AVHRR, SENTINEL, AMSR-E, AATSR, VIRR), MODIS is considered the most suitable data source for LST monitoring due to its high observation frequency, moderate spatial resolution, and free availability. This study used NASA MODIS /VIIRS Land Products Global Subsetting Tool at the ORNL DAAC, MOD11A2 LST_Day_1 km and MOD11A2 LST_Night_1 km collected within 8 days [86,87] provide time series LST data for the Tokyo metropolitan area. Several studies found that the root mean square error (RMSE) of the MODIS LST data is within 2.0 °C and exhibits high accuracy in the major global cities [88].

(3) MODIS AOD data. NASA (National Aeronautics and Space Administration)- Giovanni portal (Geospatial Interactive Online Visualization and Analysis Infrastructure) supplied the daily mean and monthly mean of total Aerosol Optical Depth at 550 nm data (MODIS Terra -AOD) [89].

(4) Air quality data. AQICN (World Air Quality Index) [90] and local monitoring networks supplied the daily mean time series data for air pollutant concentrations.

(5) Potential climate driving factors. This study used the daily mean time series of climate data (air temperature -T at 2 m height, air maximum air temperature at 2 m height, air relative humidity -RH, air pressure -p, wind speed intensity-w and direction, planetary boundary layer height -PBL) provided by MERRA-2 Version 2 (Modern-Era Retrospective Analysis for Research and Applications) [91], and C3S (Copernicus Climate Change Service) [92].

2.6. Used methodology

The UHIs phenomena are quantified using multiple indices based on either land surface temperature (LST) or air temperature. There is an imperative need for UHIs' quantification for its optimization to mitigate the increasing possible health and economic hazards. For UHI analysis, this study uses a land surface-based UHI index [9,10,93], described by equation (1):

$$\Delta LST = LST_{urban} - LST_{rural} \quad (1)$$

where ΔLST is the difference in land surface temperature of a central urbanized sector of Tokyo (LST_{urban}) and that of a representative rural area (LST_{rural}), located in a vegetated area of the metropolitan region (Fig. 1).

As the most important predictor of heat-related fatalities [48], this study used daily maximum temperatures, having the advantage of accounting for local differences in Tokyo urban climatology [5].

Current research used a robust methodology to investigate the complex interplay of COVID-19 and urban heat comprehensively, incorporating time series data analysis, an approach less commonly employed in epidemiological contexts. Cross-correlation analysis was employed to assess the similarity between two time series data of the outdoor daily mean air pollutants (PM2.5, PM10, O_3, NO_2) concentrations, the daily mean AOD levels, climate parameters (TA, T_{max}, RH, w, GHI, PBL), and COVID-19 incidence and lethality in Tokyo. Standard statistical tools, Spearman rank-correlation, rank-correlation non-parametric test coefficients, and linear regression analysis have been used for the dependence between pairs of the daily mean time series data. The primary independent variable was the maximum daily air temperature at 2 m height. Also, 8 Days of MOD11A2 LST land surface temperature LST Day/Night was used for heat waves assessment to urban heat island phenomena. Kolmogorov-Smirnov Tests of Normality have been used to assess the normality of the daily mean time-series data sets because DNC COVID-19 incidence cases and DND COVID-19 cases have a non-normal distribution. Spearman rank correlation as a nonparametric measure was chosen to identify the dependence between the rankings of the important pairs of variables. To determine the statistical significance of the correlation, we used the p-value ($p < 0.05$). ORIGIN 10.0 software version 2021 for Microsoft Windows, and ENVI 5.7 were used for data processing. All-time series data sets were preprocessed using the TIMESAT 3.2 software. Various preprocessing levels are tested, including smoothing and phenometrics computation.

3. Results

3.1. Air pollution and climate parameters impacts on COVID-19 during summer periods 2020-2022 in Tokyo

During 1 March 2020 and 1 February 2023, the Tokyo metropolis in Japan passed through eight waves of COVID-19 viral infection with the highest incidence and mortality rates under the 7th COVID-19 wave of the 2022 summer as Fig. 2 shows. It is well recognized that urban heat waves are of great concern, especially during summer in large cities, because of physiological, psychological, and health impacts and vulnerability to heat stress. For hot summers, various pre-pandemic studies reported strong correlations between at-the-ground high levels of PM2.5 and O_3 concentrations and heat stress mortality due to cardiorespiratory diseases and existing comorbidities. In urban agglomerated regions, clusters of aerosols (particulate matter and pollutant gases) can attach bioaerosols like viruses, bacteria, and fungi originating from anthropogenic or natural sources that can reach the upper and lower airways, and the lung parenchyma [82]. Also, long-term human exposure to heat waves may increase the harmful effects of air pollutants, among which the increased ground level O_3 concentrations are formed due to high solar irradiance and high temperature. The basic idea of this analysis was to compare the cumulative numbers of the daily new COVID-19 cases and daily new COVID-19 deaths during 2020-2022 per a three-month window (July-September) period and the corresponding average of daily mean of air pollutants (PM2.5, PM10, O_3, and NO_2) concentrations, total Aerosol Optical Depth at 550 nm and planetary boundary layer heights (Table 1), as well as together climate parameters variability (air temperature at 2 m height, maximum air temperature T_{max}, air pressure, wind speed intensity, surface solar irradiance), (Table 2).

In 2022, Japan experienced the hottest summer on record, with highly extreme temperatures and several consecutive heat wave events for several days and widespread areas [2,94]. Despite similar restrictions during the summers of 2020 and 2021, persistent heat waves recorded in the summer of 2022 in Tokyo linked to atmospheric dynamic changes and synergy of HWs with UHIs had severe impacts on COVID-19 viral infection transmission including excess incidence and lethality of COVID-19 cases in comparison with the previous pandemic years (Table 1). As Fig. 3 shows, in the summer of 2022, there were slight increases in the monthly ground-level concentrations of air particulate matter PM2.5.

Additionally, the moderately increased ground-level ozone concentrations during the summer of 2022 could pose a high risk for human health and intensify the greenhouse effect, with a direct impact on the intensity of the 7th COVID-19 wave. This finding confirms the results of another study [93], which reported for the summer of 2022 moderate air pollution (PM2.5, PM10, O_3, and NO_2) sources in about a 100 km radius of the Tokyo metropolitan area. However, under hot summers the mortality of people with comorbidities is increased under air pollution [95]. As Table 1 presents, due to several imposed restrictions for city traffic and local industries, the total AOD at 550 nm, which quantifies the concentration of aerosols present in the atmosphere, shows a slight decrease during summer 2022 in comparison with the previous pandemic years 2020 and 2021.

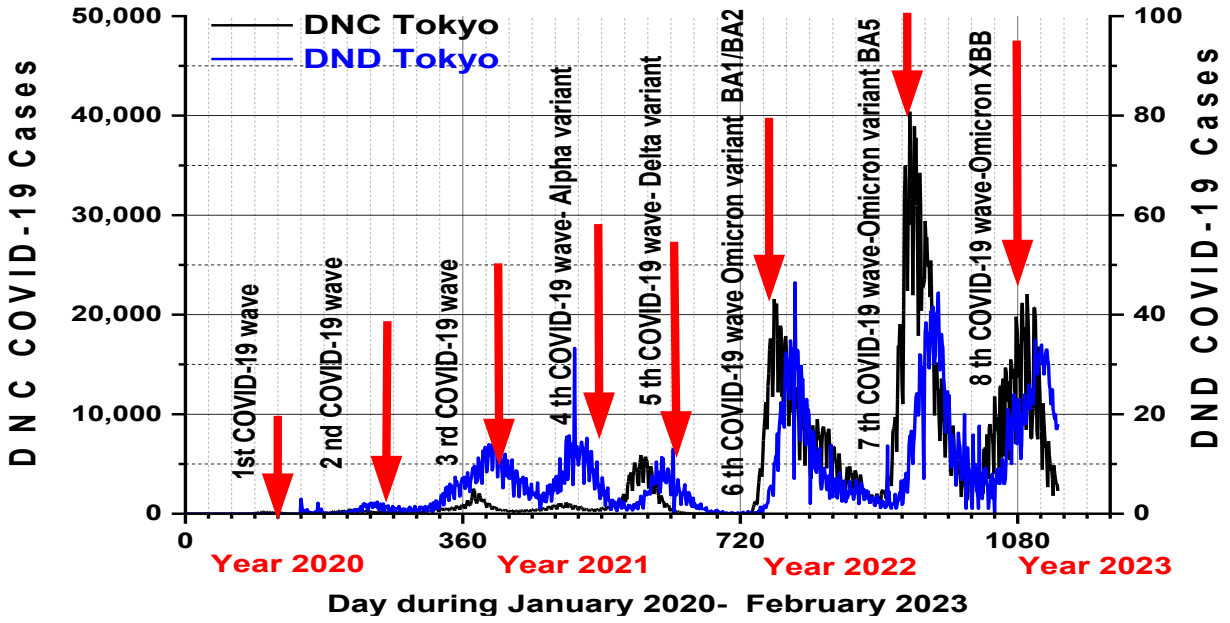

Fig. 2. Temporal pattern of COVID-19 multi waves daily new cases (DNC) and daily new deaths (DND) evolution during January 2020 and February 2023 (colour online)

Table 1. Comparative analysis of the DNC and DND COVID-19 cases for (July-September) summer periods, and the average daily mean concentrations ± standard deviations of the main air pollutants at the ground level, PBL heights, and AOD during 2020 –2022 in Tokyo metropolis.

Time period	DNC cases	DND cases	Average Daily mean ± SD PM2.5 (μg/m^3)	Average Daily mean ± SD PM10 (μg/m^3)	Average Daily mean ± SD O_3 (μg/m^3)	Average Daily mean ± SD NO_2 (μg/m^3)	Average Daily mean ± SD AOD	Average Daily mean ± SD PBL height (m)
July-September 2020	19,756	77	15.19±7.12	48.32±20.37	28.19±16.23	8.75±3.47	0.35±0.15	651.63±104.29
July-September 2021	205,794	378	13.21±7.45	47.83±18.27	29.18±12.63	8.69±4.23	0.33±0.13	651.12±49.54
July-September 2022	1,584,931	1,722	16.89±7.73	42.81±14.21	32.12±15.27	8.53±8.26	0.31±0.11	628.31±27.12

Table 2. Comparative analysis of the average daily mean climate parameters per (July-September) periods, during 2020 –2022 in Tokyo metropolitan city.

Period	Average daily mean ± SD T (°C)	Average daily mean ± SD T_{max} (°C)	Average daily mean ± SD RH (%)	Average daily mean ± SD P (hPa)	Average daily mean ± SD w (m/s)	Average daily mean ± SD GHI (W/m^2)	Average daily mean ± SD RR (mm)
July-September 2020	25.24±2.85 In the range 17.25 – 30.32	29.5 ±3.92 In the range 21.11 -37.2	82.31±4.03 In the range 74.13 – 90.47	997.48 ± 3.02 In the range 986.1 ±1002.83	3.29±2.08 In the range 0.29-9.43	292.55 ± 30.89 In the range 236.08-339.05	6.63±8.56 In the range 0.05-44.9
July-September 2021	24.52±2.63 In the range 18.47-28.51	28.54±3.94 In the range 21.11-35	82.30±4.86 In the range 70.72-91.52	998.20±4.97 In the range 985.85-1010.17	2.75±1.6 In the range 0.46-11.54	291.8±32.87 In the range 220.59-338.58	10.05±14.82 In the range 0.02-70.0
July-September 2022	25.96±2.43 In the range 18.67-31.46	30.97±2.29 In the range 25,1- 36.25	80.97±4.37 In the range 71.71-91.1	993.76±3.12 In the range 984.66-1005.12	3.37±1.69 In the range 3.09-9.39	295.67±32.26 In the range 228.17-343.51	6.95±11.35 In the range 0.01-61.74

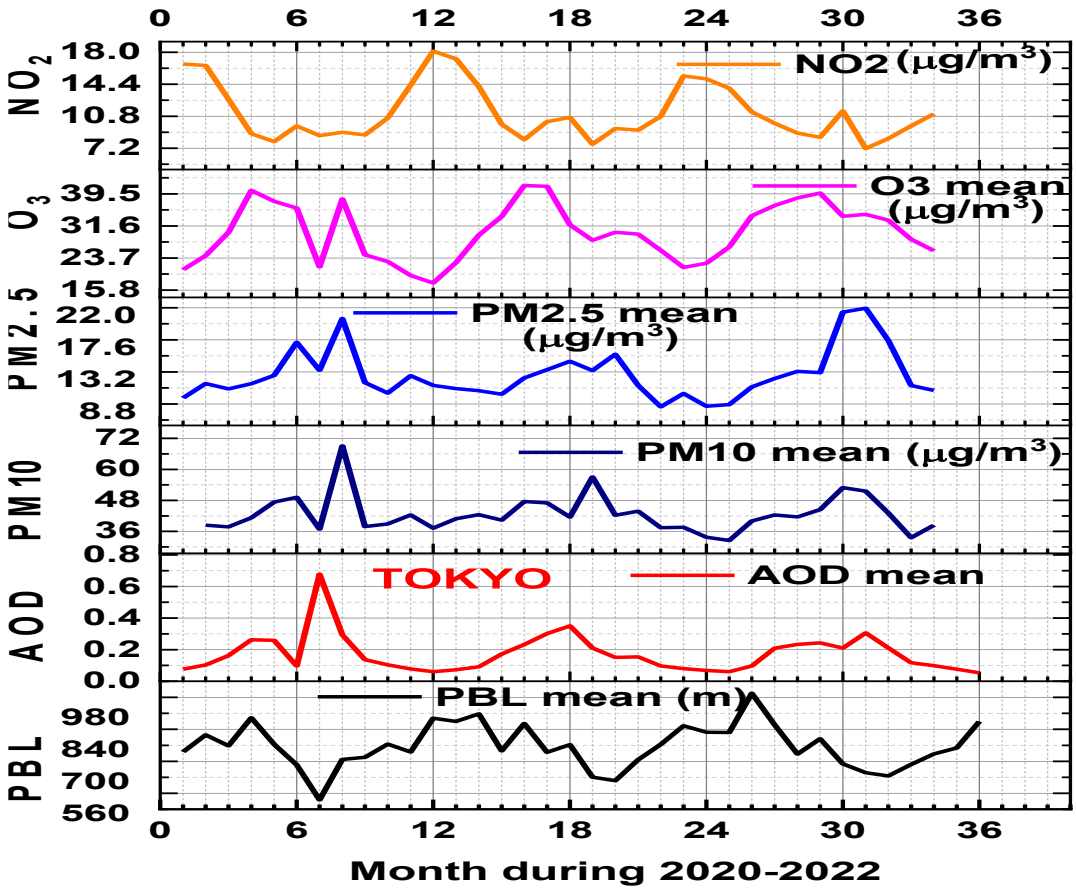

Fig. 3. Temporal pattern of the monthly air pollutant concentrations and planetary boundary layer heights in Tokyo during January 2020 - December 2022 (colour online)

Considering PM2.5 as a main potential airborne transmitter of COVID-19 pathogens via modulating the expression of angiotensin-converting enzyme ACE2 in lung injury [96], the high average of daily mean PM2.5 concentrations in value of (16.89 ± 7.73) μg/m^3 and the high value of PM2.5/PM10 ratio (0.39) showing the predominance of PM2.5 traffic-related air pollutants relative to PM10 emissions due to industries under the summer of 7th COVID-19 wave period, together with lower levels of PBL heights, may explain the high rates of total DNC cases (1,584,931), and total DND deaths (1,722) in Tokyo. Besides inhalation of indoor and outdoor virus-laden particles, high levels of average daily mean ground-level O_3 (32.12 ± 15.27) μg/m^3 attributed to the increased air temperatures and strong ultraviolet radiation recorded in Tokyo during the same period modified different immune defense responses against viral and bacterial infections. Like air pollution, outdoor-specific local meteorological factors can be top predictors of airborne viral infection spreading.

Under similar climate average values of daily mean global horizontal solar irradiance, high daily mean air temperature at 2 m height, low air pressure, low wind speed intensity, low rate of precipitations, low levels of planetary boundary layer heights recorded during the summers of 2020 to 2022, significant differences were registered for the increased values of daily maximum air temperature (30.97 ± 2.29) °C, and the decreased values of air relative humidity (80.97 ± 4.37) % during the hot summer of 2022 in Tokyo. The moderately increased values of the ground-level average daily mean particulate matter PM2.5 and ozone O_3, and maximum air temperature, together lack an Emergency State, can be additional factors contributing to the increased rates of COVID-19 incidence and mortality recorded during the summer of 2022.

Furthermore, the density of the elderly population is highly concentrated in the Tokyo prefecture, where in September 2022, people over 65 years old counted 3.12 million, which is still growing [95].

Three months-long time PBL very low heights with a mean of (628.31 ± 27.12) m, as is reflected in Fig. 4, had a great contribution to the accumulation of viral pathogens together with aerosols in the near-ground atmosphere. Considering people's vulnerability to the co-occurrence of viral infections and extreme heat, it is an urgent task to reduce heat-related risk in Tokyo.

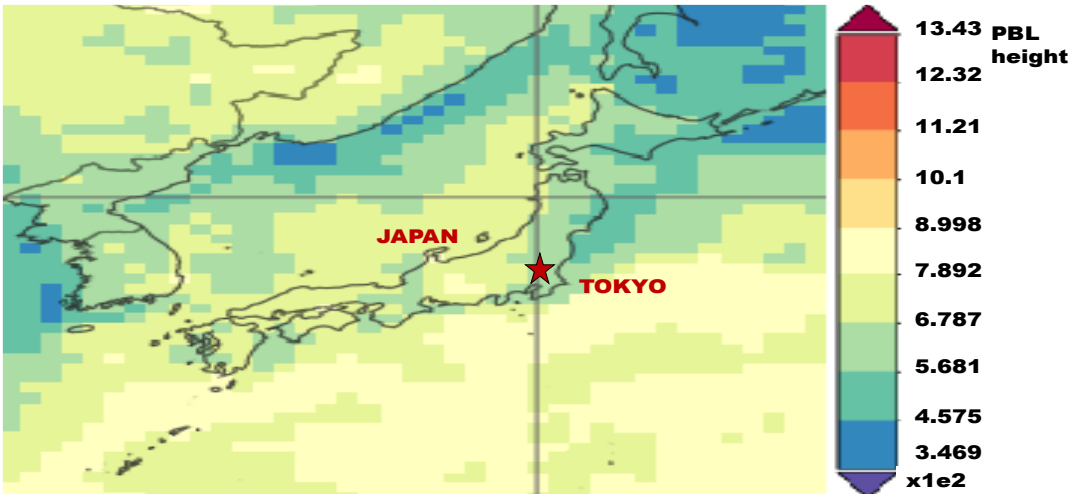

Fig. 4. Time Averaged Map of monthly planetary boundary layer PBL height (m), based on MODIS Terra data and MERRA-2 Model M2TMNXFLX v.5.12.4, over July-September 2022 in Tokyo (colour online)

3.2. Spatiotemporal patterns of LST and UHI

From MODIS11A2 Terra LST_Day_1 km and MODIS11A2 Terra LST_Night_1 km collected within 8-day period of satellite time series data analysis during 2020- 2022 COVID-19 period, the current research found for the July-September 2022 time window the highest values of land surface temperatures (LST) recorded during the day with an 8 days LST mean of (40.39 ± 2.67) °C , in the range of (35.79 - 44.23) °C. Fig. 5 comparatively illustrates temporal patterns of MODIS LST_Day and LST_Night in the central Tokyo metropolitan area during January 2020 - December 2022. Besides the seasonal and annual differences of LST, this figure shows a significant difference between diurnal and nocturnal values of LST, especially for the 2022 year. We identified LST_Day anomalies related to HWs of summer 2022.

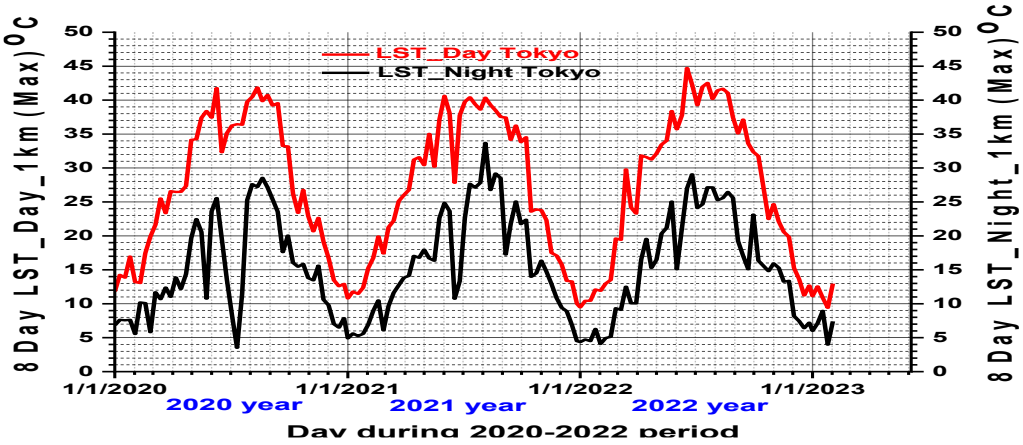

Fig. 5. Temporal patterns of MODIS LST_Day and LST_Night in the central Tokyo metropolitan area during January 2020 - December 2022 (colour online)

To curb the rate of COVID-19 infectivity, during 2020–2022-time windows in Tokyo have been implemented five states of emergencies, periods which are very well reflected by sharp sudden drops of LST_Night, and lower reductions in LST_Day in Fig. 5. Also, the imposed lockdown and partial lockdowns through states of emergencies, resulted in UHIs reduction levels (Fig. 6). Comparative analysis of summers 2020, 2021, and 2022 in Fig. 6 reveals the maximum UHI_Day value recorded during summer 2022, in comparison with the previous two summers, more intense than nocturnal UHI. Association with existing HWs, can explain the high increase in daily new incidence (DNC) and deaths (DND) of COVID-19 cases.

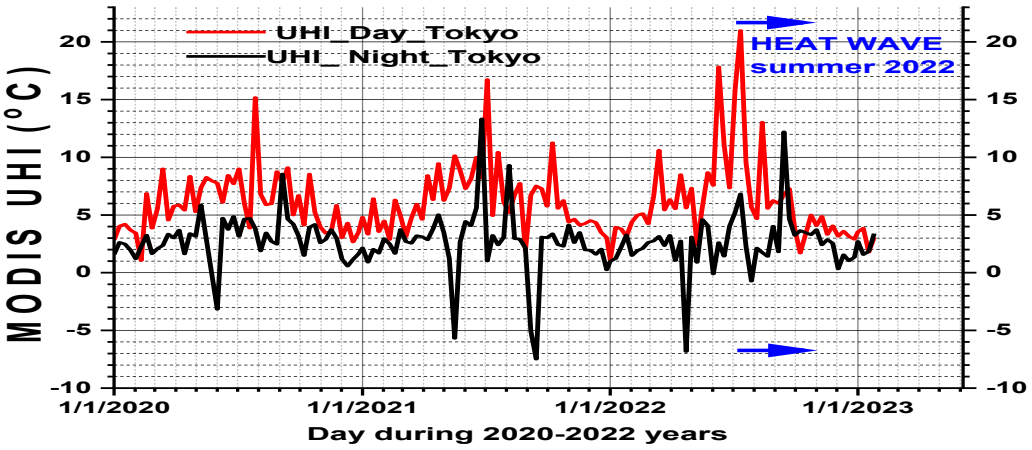

Fig. 6. Temporal patterns of MODIS UHI_Day (in red) and UHI_Night (in black) in Tokyo metropolitan area during January 2020 - December 2022 (colour online)

As Table 3 shows, there is a strong correlation between daily maximum air temperature T_{max} and daily mean global horizontal surface solar irradiance -GHI ($r = 0.82$; $p \leq 0.05$), as well as between MODIS LST_ Day max and GHI ($r = 0.91$; $p \leq 0.05$), which may illustrate the important role of surface solar irradiance involved in heat stress in Tokyo metropolis. Direct exposure of a person to solar radiation contributes significantly to much more heat than someone staying in the shade. Fig. 7 presenting the temporal evolution of the daily T_{max} and 8 days LST max MODIS in the Tokyo metropolitan area during the investigated period January 2020 - December 2022 shows a clear rise of MODIS 8 days LSTmax during summer 2022. Time series MODIS11A2 Terra LST_Night_1 km satellite data for July-September 2022 show 8 days LST mean of (25.97 ± 2.37) °C value, in the range of (21.79 - 29.54) °C, corresponding to the 7th COVID -19 wave recorded in Tokyo metropolitan area. Also, this study reports the highest value of the maximum LST_Day_1 km of 42 °C ever recorded from the 2002 year in Tokyo. There is a strong positive correlation between UHI_Day _Tokyo and LST_Day ($r = 0.79$; $p \leq 0.05$), and a lower positive correlation between UHI_Night _Tokyo and LST_Night ($r = 0.31$; $p \leq 0.05$), during the entire investigated period 2020-2022. During 1 January 2020 and 27 December 2022, MODIS UHI_Day recorded a mean value of (6.09 ± 2.69) °C, in the range (5.68 - 21.88) °C, while MODIS UHI_Night had a mean value of (2.94 ± 1.51) °C, in the range (-5.34 - 9.66) °C.

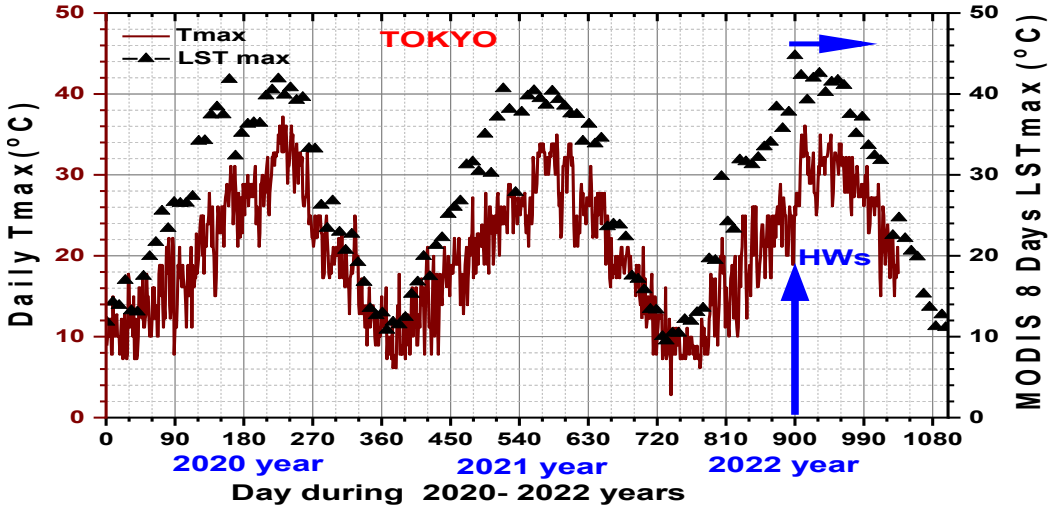

Fig. 7. Temporal patterns of daily T_{max} and 8 days LST max MODIS in Tokyo metropolitan area during January 2020 - December 2022 (colour online)

Because, land surface temperature (LST) is a key parameter related to surface-atmosphere interactions, it provides useful information for urban thermal environment patterns in Tokyo, and their trends of urban heat across city scales. Like this study, LST has been widely used for different scientific studies, such as climatology, public health, and environmental sciences [96-98]. However, LST alone cannot comprehensively capture human heat stress on the ground, which is influenced by local climate and anthropogenic factors. Urban thermal environment

parameters described in this research (T mean, T_{max}, LST_Day max) are close related to air pollutants concentrations, and climate parameters, such as global horizontal solar surface irradiance (GHI), air relative humidity (RH), air pressure, PBL height, wind speed intensity (w) and direction, and many other factors. For July 2022- September 2022 period characterized by high thermal anomaly, the findings in Table 3 present high positive Spearman statistical correlations between air T_{max} and COVID-19 incidence and lethality cases, expressed by DNC ($r = 0.81$; $p \leq 0.05$) and respectively DND ($r = 0.38$; $p \leq 0.05$). Like other study reported [99], the findings of this study consider that a rise in the air temperature, particularly during summer HWs events in the Tokyo metropolitan area, can increase the stability of viral infection, pathogen viability, and transmission of COVID-19.

Table 3. Spearman correlation coefficients and p values, between daily air mean temperature T, maximum T_{max}, and 8-day LST-Day max with the daily mean air pollutants and meteorological parameters, and with DNC and DND COVID-19 cases, for Tokyo metropolis during the 7th COVID-19 wave (July 2022-- September 2022)

Tokyo metropolis	PM2.5 ($\mu g/m^3$)	PM10 ($\mu g/m^3$)	AOD	O_3 ($\mu g/m^3$)	NO_2 ($\mu g/m^3$)	PBL (m)	RR (mm)	RH (%)	w (m/s)	P (hPa)	GHI (W/m^2)	DNC	DND
T(mean)	0.73*	0.52*	0.65*	0.30*	-0.74*	-0.83*	0.73*	0.81*	-0.19*	-0.69*	0.77*	0.21*	0.23*
T_{max}	0.49*	0.37*	0.54*	0.26*	-0.39*	-0.89*	0.94*	0.49*	-0.27*	-0.47*	0.82*	0.81*	0.38*
MODIS LST_Day max	0.62*	0.43*	0.66*	0.47*	-0.49*	-0.52*	0.95*	0.55*	-0.29*	-0.49*	0.91*	0.39*	0.18**

Note: * indicate $p \leq 0.05$, ** indicate $p \geq 0.05$.

3.3. Urban heat stress, climate variability and COVID-19 in Tokyo

Function of local climate zones, due to the cumulative effects of rapid urbanization and climate warming, during the summer period of 2022, the Tokyo metropolitan region was faced with the co-occurrence of strong HWs, UHIs, and COVID-19 viral infection. This synergistic exposure to urban heat of Tokyo inhabitants enhanced heat stress in the central Tokyo and its surrounding areas, and exacerbated the COVID-19 disease incidence and mortality [100]. However, the co-occurrence of HWs and UHIs' effects on human health shows different degrees of synergistic interactions with climate and air pollution variability, depending on several factors among which, the geographical locations of the city, the time of day, the population density, and its mobility patterns.

Under the COVID-19 pandemic period and in particular during severe hot days of summer 2022, the synergy of UHIs and HWs was responsible for the recorded high peaks of DNC and DND cases in the Tokyo metropolitan region, when the number of DND cases increased by 7.7 times than in the summer of 2021, and 80.2 times than in the summer of 2020.

To explain the highest rates of COVID-19 DNC and DND cases recorded during the 7th wave period (July-September 2022), considering the additional health risk due to heat stress disorders, the results of this study confirm the findings of similar studies, according to an increase in the urban air temperature allows an increase in viral infection transmission [101,102]. Under HWs, the synoptic analysis conducted in this study during the summer of 2022 in the Tokyo metropolis shows that the low-pressure cyclonic conditions were responsible for the hot advection of the lower layer of the troposphere and air pollutants accumulation near the ground. Moreover, at Tokyo metropolitan-scale, heat and air pollutants under low dispersion across different urban/periurban shapes and winds are crucial health risks during COVID-19 viral disease, results which are consistent with previous studies [103,104]. Scientific literature recognized the UHIs and urban hot temperatures adverse impacts on human thermal comfort, energy consumption, air pollution, and global warming [105]. As a result of climate warming and rapid urbanization, urban heat attributed to the synergy of heat waves and heat islands is a critical intervention during epidemic viral diseases.

Previous studies revealed that under non-pandemic periods due to Tokyo geomorphology, during summer hot days ($T_{max} > 35$ °C) horizontal heat advection is a key factor for the observed near-surface enhanced warming and physical heating due to the increased insolation and adiabatic heating, being associated with serious heat-related illnesses [106,107]. Also, recent global heat waves highlighted the cause-effect linkage of the morbidity and mortality rates related to the urban heat environment. Current studies employed for non-pandemic periods demonstrated that heat-related illness and mortality in large cities may be linked to prolonged exposure to extremely hot temperatures, with high effects on the body's ability to regulate its temperature, resulting in heat sickness, heat stroke, and an increase in respiratory and cardiovascular emergencies [108,109]. While human heat sensitivity depends on individual health-related factors, heat exposure is a function of the thermal environment and its meteorological conditions (air humidity, wind speed intensity, and direction, solar radiation, and its reflection, absorption, and re-emission by the atmosphere and earth's surface land covers). According to several studies, to limit the negative effects of summer hot temperatures on health

during the pandemic and non-pandemic periods is imperative to implement heat health warning systems at both regional-specific thresholds as well as at the country levels, heat waves are changing viral disease dynamics in unpredictable ways [110-115].

Besides high air temperature during the summer season, other local and regional climate factors (air relative humidity, pressure, wind speed intensity, and direction, Planetary Boundary Layer heights, PBL, surface global horizontal solar irradiance, GHI), and their interannual and seasonal variability can amplify the incidence and lethality of COVID-19 cases in the urban environment. In comparison with summers 2020 and 2021, summer 2022 in Tokyo was characterized by higher levels of particulate matter, very low levels of PBL heights (Figure 3), and atmospheric stagnant conditions associated with lower mean values of air relative humidity, air pressure, wind speed intensity, and rainfall (Fig. 8).

These peculiar climate and air pollution conditions and their seasonality may also explain the recorded high rates of COVID-19 incidence and mortality cases, being known that the urban lower atmospheric system can be a significant transport vector for airborne microbiome (viral, bacterial, fungal) communities attached to particulate matter in both concentration and biodiversity [116-118]. Also, similar to other papers' results [119], this study found a positive Spearman rank correlation association ($r = 0.38$; $p \leq 0.05$) between the DNC COVID-19 cases and surface global horizontal solar irradiance (GHI). This finding was unexpected because UV solar radiation is considered to be a virus inactivation factor [120-122], as solar radiation increases vitamin D and the immune system. However, as can be seen from Fig. 8, COVID-19 and climate-driving factors have mutual seasonality patterns in Tokyo. Also, the relative lower levels values of meteorological parameters wind speed intensity, relative air humidity, air pressure and rainfall, recorded during summer 2022, in comparison with summers 2020 and 2021, may contribute at COVID-19 viral infection transmission, and the increasing rates of incidence and lethality. Like other studies [123], our study found that air pollution and climate parameters may have more impact on COVID-19 incidence during the pandemic in Tokyo, through triggering COVID-19 viral infection transmission, while synoptic atmospheric circulation patterns are related to COVID-19 wave start-up.

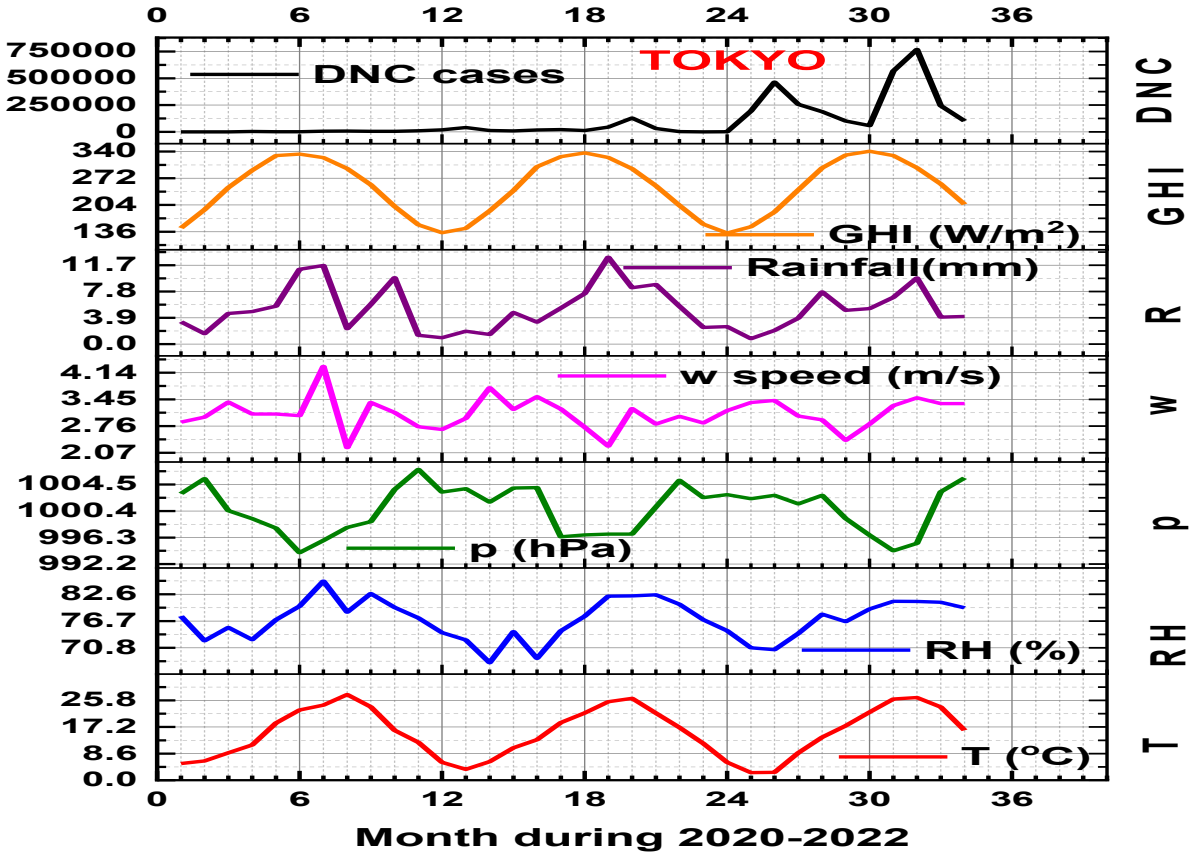

Fig. 8. Temporal patterns of the monthly climate parameters and Daily New COVID-19 cases (DNC) in Tokyo from January 2020 - December 2022 (colour online)

4. Discussion

According to the new World Health Organization Air Quality Guidelines [124], to better enhance health and promote sustainable development in large urban areas, during pandemic events overlapped with increased urban heat and air pollution concentrations, there is an urgent need to implement proper mitigation measures. It is considered that potential urban heat island (UHI) mitigation has a net beneficial effect on urban environmental quality and sustainability.

The dual impact of the urban extreme heat attributed to the increased heat stress due to the co-occurrence of UHIs, HWs associated with air pollution under the pandemic infection of COVID-19, decreased human immunity system, and further enhanced viral disease spreading and increasing lethality. However, function of the specific topography location of urban areas the transport of air pollutants emitted from the surface sources is strongly dependent on interactions between local and regional-scale atmospheric circulation. The exposure to air pollutants significantly increases with an increase in city size [125], and several air pollution episodes are responsible for strong impacts on the severity of airborne viral disease evolution and mortality [126]. Due to the significantly higher concentration of pollutants in the urban areas compared to the rural areas, aerosols (from industrial activities, vehicular traffic, and domestic practices) and ground-level ozone directly impact the UHI phenomenon [127]. Climate variables, including solar radiation, cloud cover, wind speed, and precipitation, also contribute to the formation, magnitude, and extent of UHIs. Despite the differences between air temperature at 2 m height and land surface temperature derived from satellite remote sensing data, strong correlations between them contribute to a more comprehensive global characterization of UHI effects [128]. Like other studies, this research found a relatively high increase in summer daily mean air temperature trend in the Tokyo metropolitan area during the 2020-2022 period, which may be related to long-term climate changes associated with the thermal and mechanical effects of urbanization, and a declining trend of vegetation. Rapid urbanization contributed to the conversion of urban vegetation cover to impervious areas. Tree land cover areas in Tokyo recorded a decline of 7.3 % in 2022, associated with the decreased biofilter role of green vegetation for atmospheric dust particles [129]. Some studies found the increased values of the annual mean of land surface temperature of 3 °C/century between 1901- 2015 in Tokyo [130]. Urban expansion in Tokyo during recent years led to significant increases in impervious surface land cover, contributing to pronounced LST rise and UHIs intensifying with severe health effects during COVID-19. However, vegetation land cover provides more efficient cooling than water bodies in mitigating LST during HWs across different bay areas. However, Tokyo's annual mean air temperature has an increasing trend, which shows the progress of global warming. For non-pandemic periods in Tokyo, and 2 °C global climate warming scenarios were estimated to have an increase in the daily heat illness in the 2040s, twice that in the 2010s [131]. Considering this forecasting, during a future viral epidemic event, the daily incidence and lethality of viral diseases will be enhanced. Besides urban heat stress and other meteorological factors, COVID-19 hotspot analysis of population movements and social events in Japan contributed to the spreading of SARS-CoV-2 viral infections [132,133].

The intensification of the globalization process associated with urban land cover expansion, together with the increasing trend of sustainable development, is responsible for several changes in highly urbanized areas with a high impact on the urban thermal environment. Because urban extreme summer heat is an increasingly prevalent hazard worldwide as well as in Tokyo metropolises, urban planners must consider heat vulnerability reduction by adopting policies related to preserving and creating green-blue spaces and environmental sustainability performance [134,135]. To mitigate the UHI effects on summer hot thermal environment and reduce energy consumption, some studies demonstrated the need to integrate green spaces between high-rise buildings in big cities [136-141]. Urban green mitigates urban heat by altering evapo-transpiration processes and providing cooling effects to the surrounding environment [142,143]. Based on monthly derived land surface temperature from MODIS Terra imagery was reported that through implementing heat stress mitigation measures, summer heat-related illnesses decreased during (June–September) month from 2000 to 2022 by 3.2 in seven large cities in California, US [144]. Some recent urban heat stress studies [145-147] employed various novel approaches, using heat thresholds based on higher spatial resolution, including Landsat-9 [148] and Sentinel 3 [149] satellite remote sensing data. The response of UHIs during HW events varies with different conditions (HW intensity, frequency, and maximum duration, day-and-night contrast, and microclimate zones). To protect people's health and well-being, there is an urgent need for the development and implementation of urban information environmental integrated systems and forecasting models for air pollutants dispersion during stagnant weather conditions for the assessment of the thermal stress impact on health, particularly for hot summers worldwide [150-153].

In good accordance with other studies [154,155], this study considers that ongoing global warming could hinder people's use of urban green spaces during summer hot periods during pandemic events. The novelty of this paper is to connect the COVID-19 pandemic and the summer 2022 high temperature in the Tokyo metropolitan region more comprehensively, providing urban decision-makers and planners with references for heat mitigation, prevention, and adaptation strategies of sustainable development.

A recent study [156] found that in non-pandemic summers, assuming current vulnerability and socioeconomic structures remain unchanged, heat-related

mortality levels in Tokyo can reach COVID-19 mortality in less than ten years at a + 3.0 °C increase in global warming relative to preindustrial era. Rapid climate action is needed to curb these projected levels. Under global climate warming, the transmission and spread of vector-borne diseases (VBDs) like as COVID-19 will be a major threat to human health in the future [157], and heat waves will accelerate the spread of infectious diseases [158].

5. Conclusion

Based on a comprehensive analysis of air pollution and climate variability trends, this research focused on the hotspots of COVID-19 infections in the Tokyo metropolitan area during the summers of 2020, 2021, and 2022. This study revealed the relationship between UHI and HW associated with air pollution under low-pressure cyclonic conditions and lower levels of PBL heights during the COVID-19 pandemic event in the Tokyo metropolitan area and highlighted the summer 2022 extreme HWs effects on increased incidence and lethality rates of COVID-19 viral infection disease. Also, the findings of this study suggest that remote sensing MODIS satellite data can be effectively used to analyze the thermal environment impact on viral infection trends in densely populated urban areas. The results highlight the direct effects of air pollution and local meteorological synoptical conditions in the spreading and exacerbating health risks of pandemic viral infections in large metropolitan areas, particularly in Tokyo. Additionally, this study considers the significant contribution of urban heat stress attributed to persistent summer heat waves associated with urban heat island phenomena on COVID-19 incidence and lethality, which requires interventional measures of urban decision-makers to enhance air quality and efficient control of epidemic disease, especially in highly exposed population groups with comorbidities.

To develop a sustainable approach to minimize the UHI and HWs effects on viral infection transmission during summer hot periods and improve urban resilience, decision-makers must implement efficient prevention and mitigation actions. In the frame of global warming is essential to adopt proper strategies for the reduction of air pollution under HWs periods, for optimizing the design of urban thermal environments that limit the negative impacts of climate extremes on people's health. The results of this paper can help epidemiologists understand the behaviour of viral infection against environmental variables, helping healthcare policymakers combat the COVID-19 pandemic and control future epidemic threats in agglomerated cities. This study may offer a scientific basis to formulate area-specific heat adaptation strategies for urban planning, clean production, and human health. It is crucial to anticipate the most serious threats of climate warming over the coming decades and to support mitigation and adaptation efforts tailored to urban and regional needs during heat waves and pandemic events.

Achieving the Sustainable Development Goals (SDGs) 2030 requires implementing urgent strategies for reducing air pollution and extreme heat events adverse effects on human health. Such studies will be useful for understanding future transmission dynamics and lethality of other infectious diseases during hot summers in big cities worldwide. However, the complexities of sustainable urban development imply a complex analysis of several factors, including urbanization rate, spatiotemporal land cover changes, urban green infrastructure, air pollution and climate variability, natural and anthropogenic hazards, and geographic and socioeconomic conditions.

Acknowledgements

This study was supported by the Romanian Ministry of Education and Research, Research Development and Innovation Plan 2022-2027, CONTRACT PN 23 05 NUCLEU; We are very thankful to the NASA MODIS products, and MERRA-2 derived meteorological and solar parameters product provided by the Copernicus Atmosphere Monitoring Service (CAMS).

References

[1] CDC, https://covid.cdc.gov/covid-data-tracker/#variant-proportions
[2] JMA, (2022). JMA Report TCC News, Autumn 2022.
[3] C. Zong, Applied and Computational Engineering **7**, 302 (2023).
[4] C. Wei, W. Chen, Y. Lu, T. Blaschke, J. Peng, D. Xue, Remote Sens. **14**, 70 (2022).
[5] G. Chen, Y. Chen, H. He, J. Wang, L. Zhao, Y. Cai, Building and Environment **240**, 110434 (2023).
[6] A. Alari, N. Letellier, T. Benmarhnia, Science of the Total Environment **892**, 164543 (2023).
[7] Y. Du, J. Xie, Z. Xie, N. Wang, L. Zhang, Remote Sensing **17**, 892 (2025).
[8] X. Zhang, Y. Liu, R. Chen, M. Si, C. Zhang, Y. Tian, G. Shang, Remote Sensing **17**, 781 (2025).
[9] J. Liu, Y. Ren, H. Tao, M. J. Shalamzari, Remote Sensing **13**(19), 3824 (2021).
[10] P. Shen, S. Zhao, D. Zhou, B. Lu, Z. Han, Y. Ma, Y. Wang, C. Zhang, C. Shi, L. Song, Z. Pan, Z. Li, S. Liu, Science of the Total Environment, **955**, 177035 (2024).
[11] A. Kumar, M. Mukherjee, A. Goswami, Remote Sensing Applications: Society and Environment **30**, 100970 (2023).
[12] L. Yang, Q. Li Qi, L. Zhao, Z. Luo, iScience **27**(3), 108863 (2024).
[13] N. Nour Eldeen, K. Mao, Z. Yuan, X. Shen, T. Xu, Z. Qin, Remote Sensing **12**, 488 (2020).
[14] T. N. Phan, M. Kappas, K. T. Nguyen, T. P. Tran, Q. V. Tran, A. R. Emam, International Journal of Remote Sensing **40**, 5544 (2019).
[15] B. Wei, Y. Bao, S. Yu, S. Yin, Y. Zhang, International Journal of Applied Earth Observation and Geoinformation **100**, 102342 (2021).
[16] Z. Wang, Y. Liu, T. Wang, S. Tang, X. Wu, Urban Climate **60**, 102356 (2025).

[17] Z. Wu, Y. Wang, Y. Ren, Landscape and Urban Planning **257**, 105314 (2025).
[18] A. Esposito, G. Pappaccogli, A. Donateo, P. Salizzoni, G. Mafeis, T. Semeraro, J. L. Santiago, R. Buccolieri, Remote Sensing **16**, 4496 (2024).
[19] M. Zoran, D. Savastru, M. N. Tautan, L. Baschir, J. Optoelectron. Adv. M. **21**(7-8), 470 (2019).
[20] P. Shen, S. Zhao, D. Zhou, B. Lu, Z. Han, Y. Ma, Y. Wang, C. Zhang, C. Shi, L. Song, Z. Pan, Z. Li, S. Liu, Science of the Total Environment **955**, 177035 (2024).
[21] B. J. He, Urban Climate **24**, 26 (2018).
[22] A. Gupta, B. De, S. Das, M. Mukherjee, Urban Climate **59**, 102296 (2025).
[23] M. Quick, Health Reports **35**(6), 3 (2024).
[24] L. Niu, Z. Zhang, Y. Liang, J. van Vliet, Environment International **184**,108455 (2024).
[25] M. M. Patwary, A. S. Disha, D. Sikder, S. Hasan, J. Hossan, M. Bardhan, S. M. Billah, Me. Hasan, Ma. Hasan, Md Z. Haque, S. Al Imran, Md P. Kabir, Md N. S. Pitol, M. R. Ritu, C. Saha, M. H. E. M. Browning, Md Salahuddin, International Journal of Disaster Risk Reduction **116**, 105066 (2025).
[26] C. Y. Wai, N. Muttil, M. A. U. R. Tariq, P. Paresi, R. C. Nnachi, A. W. M. Ng, Sustainability **14**, 378 (2022).
[27] P. L. C. Chua, Y. Takane, C. F. S. Ng, K. Oka, Y. Honda, Y. Kim, M. Hashizume, Environment International **181**, 108310 (2023).
[28] M. Rai, M. Stafoggia, F. de'Donato, M. Scortichini, S. Zafeiratou, L. Vazquez Fernandez, S. Zhang, K. Katsouyanni, E. Samoli, S. Rao, E. Lavigne, Y. Guo, H. Kan, S. Osorio, J. Kyselý, A. Urban, H. Orru, M. Maasikmets, J. J. K. Jaakkola, N. Ryti, S. Breitner, Environment International **174**, 107825 (2023).
[29] J. Ballester, M. Quijal-Zamorano, R. F. Méndez Turrubiates, F. Pegenaute, F. R. Herrmann, J. M. Robine, X. Basagaña, C. Tonne, J. M. Antó, H. Achebak, Nature Medicine **29**, 1857 (2023).
[30] L. J. Harrington, D. Frame, Climatic Change **174**, 2 (2022).
[31] S. Lüthi, C. Fairless, E. M. Fischer, N. Scovronick, B. Armstrong, M. De Sousa Zanotti Stagliorio Coelho, Y. L. Guo, Y. Guo, Y. Honda, V. Huber, J. Kyselý, E. Lavigne, D. Royé, N. Ryti, S. Silva, A. Urban, A. Gasparrini, D. N. Bresch, A. M. Vicedo-Cabrera, Nature Communications **14**, 4894 (2023).
[32] A. M. Vicedo-Cabrera, N. Scovronick, F. Sera, D. Royé, R. Schneider, A. Tobias, C. Astrom, Y. Guo, Y. Honda, D. M. Hondula, R. Abrutzky, S. Tong, M. de Sousa Zanotti Stagliorio Coelho, P. H. Nascimento Saldiva, E. Lavigne, P. Matus Correa, N. Valdes Ortega, H. Kan, S. Osorio, J. Kyselý, A. Urban, H. Orru, E. Indermitte, J. J. K. Jaakkola, N. Ryti, M. Pascal, A. Schneider, K. Katsouyanni, E. Samoli, F. Mayvaneh, A. Entezari, P. Goodman, A. Zeka, P. Michelozzi, F. de'Donato, M. Hashizume, B. Alahmad, M. Hurtado Diaz, C. De La Cruz Valencia, A. Overcenco, D. Houthuijs, C. Ameling, S. Rao, F. Di Ruscio, G. Carrasco-Escobar, X. Seposo, S. Silva, J. Madureira, I. H. Holobaca, S. Fratianni, F. Acquaotta, H. Kim, W. Lee, C. Iniguez, B. Forsberg, M. S. Ragettli, Y. L. L. Guo, B. Y. Chen, S. Li, B. Armstrong, A. Aleman, A. Zanobetti, J. Schwartz, T. N. Dang, D. V. Dung, N. Gillett, A. Haines, M. Mengel, V. Huber, A. Gasparrini, Nature Climate Change **11**, 492 (2021).
[33] D. Xi, L. Liu, M. Zhang, C. Huang, K. G. Burkart, K. Ebi, Y. Zeng, J. S. Ji, Nature Medicine **30**, 1489 (2024).
[34] D. L. Schumacher, J. Singh, M. Hauser, E. M. Fischer, Martin Wild, S. I. Seneviratne, Communications Earth and Environment **5**, 182 (2024).
[35] P. M. Sousa, R. M. Trigo, A. Russo, J. L. Geirinhas, A. Rodrigues, S. Silva, A. Torres, International Journal of Biometeorology **66**, 457 (2022).
[36] A. Casanueva, S. Kotlarski, M. A. Liniger, C. Schwierz, A. M. Fischer, Climate Services **30**, 100372 (2023).
[37] IPCC, (2022). Global Warming of 1.5°C: IPCC Special Report on Impacts of Global Warming of 1.5°C above Pre-industrial Levels in Context of Strengthening Response to Climate Change, Sustainable Development, and Efforts to Eradicate Poverty (1st ed.), Cambridge University Press.
[38] R. Cole, S. Hajat, P. Murage, C. Heaviside, H. Macintyre, M. Davies, P. Wilkinson, Environment International **173**, 107836 (2023).
[39] G. Zhang, L. Han, J. Yao, J. Yang, Z. Xu, X. Cai, J. Huang, L. Pei, Front. Public Health **11**, 1 (2023).
[40] K. Oka, Y. Honda, V. L. H. Phung, Y. Hijioka, Environ. Res. **232**, 116390 (2023).
[41] T. Nishimura, E. A. Rashed, S. Kodera, H. Shirakami, R. Kawaguchi, K. Watanabe, M. Nemoto, A. Hirata, Sustain. Cities Soc. **74**, 103203 (2021).
[42] A. Takada, S. Kodera, K. Suzuki, M. Nemoto, R. Egawa, H. Takizawa, A. Hirata, Front. Public Health **11**, 1061135 (2023).
[43] H. Ueta, S. Kodera, S. Sugimoto, A. Hirata, Environmental Research **247**, 118202 (2024).
[44] M. Rai, S. Breitner, V. Huber, S. Zhang, A. Peters, A. Schneider, Environ. Res. **229**, 115668 (2023).
[45] M. Baccini, A. Biggeri, G. Accetta, T. Kosatsky, K. Katsouyanni, A. Analitis, H. R. Anderson, L. Bisanti, D. D'Ippoliti, J. Danova, B. Forsberg, S. Medina, A. Paldy, D. Rabczenko, C. Schindler, P. Michelozzi, Epidemiology **19**, 711 (2008).
[46] D. D'Ippoliti, P. Michelozzi, C. Marino, F. de'Donato, B. Menne, K. Katsouyanni, U. Kirchmayer, A. Analitis, M. Medina-Ramon,

A. Paldy, R. Atkinson, S. Kovats, L. Bisanti, A. Schneider, A. Lefranc, C. Iniguez, C. A. Perucci, Environmental Health **9**, 37 (2010).
[47] B. J. He, Urban Climate **24**, 26 (2018).
[48] D. Royé, M. T. Zarrabeitia, J. Riancho, A. Santurtún, Environmental Research **173**, 349 (2019).
[49] D. Royé, A. Figueiras, M. Taracido, Pharmacoepidemiol. Drug Saf. **27**(6), 638 (2018).
[50] M. Beniston, D. B. Stephenson, O. B. Christensen, C. A. T. Ferro, C. Frei, S. Goyette, K. Halsnaes, T. Holt, K. Jylhä, B. Koffi, J. Palutikof, R. Schöll, T. Semmler, K Woth, Climate Change **81**, 71 (2007).
[51] M. Zargari, A. Mofidi, A. Entezari, M. Baaghideh, Scientific Reports **14**, 643 (2024).
[52] L. Zhao, X. Fan, T Hong, Atmosphere **16**, 791 (2025).
[53] D. Hidalgo-García, J. Arco-Díaz, Sustain. Cities Soc. **87**, 104166 (2022).
[54] M. Zoran, R. Savastru, D. Savastru, A. Dida, O. Ionescu, Proc. of SPIE **8887**, 888720 (2013).
[55] P. K. Diem, C. T. Nguyen, N. K. Diem, N. T. H. Diep, P. T. B. Thao, T. G. Hong, T. N. Phan, Remote Sensing Applications: Society and Environment **33**, 101081 (2024).
[56] M. Zoran, R. Savastru, D. Savastru, Journal of Radioanalytical and Nuclear Chemistry **293**(2), 655 (2012).
[57] N. van Doremalen, T. Bushmaker, D. H. Morris, M. G. Holbrook, A. Gamble, B. N. Williamson, A. Tamin, J. L. Harcourt, N. J. Thornburg, S. I. Gerber, J. O. Lloyd-Smith, E. de Wit, V. J. Munster, The New England Journal of Medicine **382**(16), 1564 (2020).
[58] R. Tignat-Perrier, A. Dommergue, A. Thollot, O. Magand, P. Amato, M. Joly, K. Sellegri, T. M. Vogel, C. Larose, Science of The Total Environment **716**, 137129 (2020).
[59] M. Zoran, R. Savastru, D. Savastru, M. N. Tautan, Science of the Total Environment **738**, 139825 (2020).
[60] J. Uetake, Y. Tobo, Y. Uji., T. C J Hill, P. J. DeMott, S. M. Kreidenweis, R. Misumi, Frontiers in Microbiology **10**, 01572 (2019).
[61] H. Nishiura, N. M. Lintona, A. R. Akhmetzhanov, International Journal of Infectious Diseases **93**, 284 (2020).
[62] X. Feng, X. Xu, X. Yao, Y. Zhao, Y. Tang, Z. Zhao, Y. Wei, T. Mehmood, X.-S. Luo, Atmospheric Research **305**, 107453 (2024).
[63] J. Gong, J. Qi, E. Beibei, Y. Yin, D. Gao, Environmental Pollution **25**, 113485 (2020).
[64] M. Jin, J. M. Shepherd, W. Zheng, Advances in Meteorology **2010**, 681587 (2010).
[65] M. S. Jin, W. Kessomkiat, G. Pereira, Remote Sensing **3**, 83 (2011).
[66] V. Ramanathan, M. V. Ramana, G. Roberts, D. Kim, C. Corrigan, C. Chung, D. Winker, Nature **448**, 575 (2007).
[67] M. Santamouris, S. Haddad, M. Saliari, K. Vasilakopoulou, A. Synnefa, R. Paolini, G. Ulpiani, S. Garshasbi, F. Fiorito, Energy and Buildings **166**, 154 (2018).
[68] D. Buadong, W. Jinsart, I. Funatagawa, K. Karita, E. Yano, Journal of Epidemiology **19**(4), 182 (2009).
[69] K. Luo, R. Li, W. Li, Z. Wang, X. Ma, R. Zhang, X. Fang, Z. Wu, Y. Cao, Q. Xu, Scientific Reports **6**, 38328 (2016)
[70] A. Analitis, P. Michelozzi, D. D'Ippoliti, F. De'Donato, B. Menne, F. Matthies, R. W. Atkinson, C. Iñiguez, X. Basagaña, A. Schneider, A. Lefranc, A. Paldy, L. Bisanti, K. Katsouyanni, Epidemiology **25**(1), 15 (2014).
[71] J. L Domingo, J. Rovira, Environmental Research **187**, 109650 (2020).
[72] J. L. Domingo, M. Marques, J. Rovira, Environmental Research **188**, 109861 (2020).
[73] L. Setti, F. Passarini, G. De Gennaro, P. Barbieri, M. G. Perrone, M. Borelli, J. Palmisani, A. Di Gilio, V. Torboli, F. Fontana, L. Clemente, A. Pallavicini, M. Ruscio, P. Piscitelli, A. Miani, Environmental Research **188**, 109754 (2020).
[74] J. Shang, G. Ye, K. Shi, Y. Wan, C. Luo, H. Aihara, Q. Geng, A. Auerbach, F. Li, Nature **581**, 221 (2020).
[75] T. Ju, T. Geng, B. Li, B. An, R. Huang, J. Fan, Z. Liang, J. Duan, Sustainability **14**(24), 16720 (2022).
[76] A. Jana, S. Kundu, S. Shaw, A. Chakraborty, A. Chattopadhyay, Environmental Research **222**, 115288 (2023).
[77] Y. Liang, K. Gui, H. Che, L. Li, Y. Zheng, X. Zhang, X. Zhang, P. Zhang, X. Zhan, Science of the Total Environment **857**(Part 3), 159435 (2023).
[78] S. Ramachandran, K. Ansari, Atmospheric Environment **343**, 120948, (2025).
[79] T. Su, Z. Li, Y. Zheng, Q. Luan, J. Guo, Geophysical Research Letters **47**, 90041 (2020).
[80] E. Ceccarelli, G. I. Minell, A. Maruotti, G. J. Lasinio, M. Martuzzi, Health and Place **90**, 103357 (2024).
[81] Y. Wu, K. Zhao, J. Huang, M. Arend, B. Gross, F. Moshary, Atmospheric Environment **218**, 117024 (2019).
[82] D. Zendeli, N. Colaninno, D. Maiullari, M. van Esch, A. van Timmeren, G. Marconi, R. Bonora, E. Morello, Sustainable Cities and Society **124**, 106181 (2025).
[83] C. O'Malley, H. Kikumoto, Sustainable Cities and Society **83**, 103959 (2022).
[84] Worldometer Info. (2025). Available online: https://www.worldometers.info/.
[85] WHO, (2025), https://covid19.who.int/WHO-COVID-19-global-data.csv.
[86] NASA MODIS https://modis.ornl.gov/.
[87] ORNL, D.A.A.C., MODIS and VIIRS Land Products Global Subsetting and Visualization Tool, ORNL DAAC, Oak Ridge, Tennessee, USA (2018). https://doi.org/ 10.3334/ORNLDAAC/1379.
[88] C. Yoo, J. Im, D. Cho, N. Yokoya, J. Xia, B. Bechtel, Remote Sensing **12**, 1398 (2020).

[89] Giovanni (2025), https://giovanni.gsfc.nasa.gov/giovanni/.
[90] AQICN (2025), https://aqicn.org/city/.
[91] MERRA, (2025), http://www.soda-pro.com/web-services/meteo-data/merra.
[92] Copernicus (2025), https://cds.climate.copernicus.eu/
[93] J. Luo, Y. Yao, Q. Yin, Sensors **23**, 9206 (2023).
[94] Metro-Tokyo, https://www.metro.tokyo.lg.jp/english/index.html).
[95] A. Damiani, H. Irie, D. A. Belikov, S. Kaizuka, H. M. S. Hoque, R. R. Cordero, Atmospheric Chemistry and Physics **22**, 12705 (2022).
[96] M. Scortichini, M. De Sario, F. K. de'Donato, M. Davoli, P. Michelozzi, M. Stafoggia, Int. J. Environ. Res. Publ. Health **15**(8), 1771 (2018).
[97] M.-W. Lin, C.-H. Lin, J.-R. Chang, H.-H. Chiang, T.-H. Wu, C.-S. Lin, Journal of Hazardous Materials **485**, 136887 (2025).
[98] Y. Tian, A. Kleidon, C. Lesk, S. Zhou, X. Luo, S. A. Ghausi, G. Wang, D. Zhong, J. Zscheischler, Communications Earth and Environment **5**, 617 (2024).
[99] E. Noh, J. Kim, S.-Y. Jun, D.-H. Cha, M.-S. Park, J.-H. Kim, H.-G. Kim, Geophysical Research Letters **48**, 18 (2021).
[100] N. S. M. Harmay, M. Choi, Building and Environment **209**, 108677 (2022).
[101] M. Bhatta, E. Field, M. Cass, K. Zander, S. Guthridge, M. Brearley, S. Hines, G. Pereira, D. Nur, A. Chang, G. Singh, S. Trueck, C. Truong, J. Wakerman, S. Mathew, Climate **11**, 246 (2023).
[102] W. Wang, B.-J. He, Sustainable Cities and Society **90**, 104387 (2023).
[103] A. Pivato, G. Formenton, F. Di Maria, T. Baldovin, I. Amoruso, T. Bonato, P. Mancini, G. Bonanno Ferraro, C. Veneri, M. Iaconelli, L. Bonadonna, T. Vicenza, G. La Rosa, E. Suffredini, Int. J. Environ. Res. Publ. Health **19**(15), 9462 (2022).
[104] Y. Zhang, Y. Fan, J. Ge, Building and Environment **270**, 112530 (2025).
[105] K. Hayashida, K. Shimizu, H. Yokota, Acute Medicine and Surgery **6**(2), 206 (2019).
[106] Y. Imada, M. Watanabe, H. Kawase, H. Shiogama, M. Arai, SOLA **15**A(A), 8 (2019).
[107] Y. Iwasaki, K. Kasai, K. Hirukawa, M. Kawakami, Prehospital and Disaster Medicine **34**(s3), s29 (2019).
[108] M. Pascal, V. Wagner, A. Alari, M. Corso, A. L. Tertre, Atmospheric Environment **249**, 118249 (2021).
[109] J. Ballester, M. Quijal-Zamorano, R. F. Méndez Turrubiates, F. Pegenaute, F. R. Herrmann, J. M. Robine, X. Basagaña, C. Tonne, J. M. Antó, H. Achebak, Nature Medicine **29**, 1857 (2023).
[110] K. Pantavou, D. Piovani, S. Bonovas, G. K. Nikolopoulos, Euro-Mediterranean Journal for Environmental Integration **9**, 115 (2023).
[111] X. Lian, J. Huang, H. Li, Y. He, Z. Ouyang, S. Fu, Y. Zhao, D. Wang, R. Wang, X. Guan, Environmental Research **231**(Part 2), 116090 (2023).
[112] M. Rai, M. Stafoggia, F. de'Donato, M. Scortichini, S. Zafeiratou, L. Vazquez Fernandez, S. Zhang, K. Katsouyanni, E. Samoli, S. Rao, E. Lavigne, Y. Guo, H. Kan, S. Osorio, J. Kyselý, A. Urban, H. Orru, M. Maasikmets, J. J. K. Jaakkola, N. Ryti, M. Pascal, M. Hashizume, C. F. S. Ng, B. Alahmad, M. Hurtado Diaz, C. De la Cruz Valencia, B. Nunes, J. Madureira, N. Scovronick, R. M. Garland, H. Kim, W. Lee, A. Tobias, C. Íñiguez, B. Forsberg, C. Åström, A. M. Vicedo-Cabrera, M. S. Ragettli, Y. L. L. Guo, S. C. Pan, S. Li, A. Gasparrini, F. Sera, P. Masselot, J. Schwartz, A. Zanobetti, M. L. Bell, A. Schneider, S. Breitner, Environment International **174**, 107825 (2023).
[113] M. M. Patwary, A. S. Disha, D. Sikder, S. Hasan, J. Hossan, M. Bardhan, S. M. Billah, M. Hasan, M. Hasan, Md Z. Haque, S. Al Imran, Md P. Kabir, Md N. S. Pitol, M. Rahman Ritu, C. Saha, M. H. E. M. Browning, Md Salahuddin, International Journal of Disaster Risk Reduction **116**, 105066, (2025).
[114] A. Matzarakis, G. Laschewski, S. Muthers, Atmosphere **11**, 170 (2020).
[115] A. Matzarakis, Atmosphere **15**, 684 (2024).
[116] X. Xia, K. Zhang, R. Yang, Y. Zhang, D. Xu, K. Bai, J. Guo, Atmospheric Environment **268**, 118848 (2022).
[117] R. Tignat-Perrier, A. Dommergue, A. Thollot, O. Magand, P. Amato, M. Joly, K. Sellegri, T. M. Vogel, C. Larose, Science of the Total Environment **716**, 137129 (2020).
[118] A. Jana, S. Kundu, S. Shaw, S. Chakraborty, A. Chattopadhyay, Environmental Research **222**, 115288 (2023).
[119] L. Nottmeyer, B. Armstrong, R. Lowe, S. Abbott, S. Meakin, K. M. O'Reilly, R. von Borries, R. Schneider, D. Royé, M. Hashizume, M. Pascal, A. Tobias, A. M. Vicedo-Cabrera, E. Lavigne, P. Matus Correa, N. Valdés Ortega, J. Kynčl, A. Urban, H. Orru, N. Ryti, F. Sera, Science of the Total Environment **854**, 158636 (2023).
[120] J. Herman, B. Biegel, L. Huang, Air Quality Atmosphere and Health **14**, 217 (2021).
[121] M. Heßling, K. Hönes, P. Vatter, C. Lingenfelder, GMS Hygiene and Infection Control **14**, 15 Doc08 (2020).
[122] M. Biasin, A. Bianco, G. Pareschi, A. Cavalleri, C. Cavatorta, C. Fenizia, P. Galli, L. Lessio, M. Lualdi, E. Tombetti, A. Ambrosi, E. M. A. Redaelli, I. Saulle, D. Trabattoni, A. Zanutta, M. Clerici, Nature Scientifc Reports **11**, 6260 (2021).
[123] A. Shinzato, K. Hibiya, K. Nishiyama, N. Ikemiyagi, W. Arakaki, W. Kami, D. Nabeya, S. Ideguchi, H. Nakamura, M. Furugen, K. Miyagi, M. Nakamatsu, S. Haranaga, T. Kinjo, J. Fujita,

K. Nakamura, K. Yamamoto, International Journal of Infectious Diseases **154**, 107833 (2025).
[124] WHO (2024), WHO Ambient Air Quality Guidelines Database, Version 6.1. Geneva, World Health Organization, 2024.
[125] X. Zhao, W. Zhou, M. Hong, A. M. Neophytou, Environmental Research **267**, 120661(2025).
[126] G. He, P. Pan, T. Tanaka, Journal of Environmental Economics and Management **130**, 103117(2025).
[127] K. S. Arunab, A. Mathew, Sustainable Cities and Society **101**, 105117 (2024).
[128] G. Suthar, S. Singh, N. Kaul, S. Khandelwal, Remote Sensing Applications: Society and Environment **35**, 101265 (2024).
[129] K. Shiraishi, T. Terada, Urban Forestry and Urban Greening **97**, 128331 (2024).
[130] J. Matsumoto, F. Fujibe, H. Takahashi, Journal of Environmental Sciences **59**, 54 (2017).
[131] Q. Zhang, Y. Guan, X. Wu, J. Zhang, R. Li, K. Lin, Y. Wang, Building and Environment **267**(Part B), 112266 (2025).
[132] A. Zaitunah, Samsuri, A. F.Silitonga, L. Syaufina, Sensors **22**(11), 4168 (2022).
[133] S. Yu, K. L. Lei, D. Li, Y. J. Kim, M. Nemoto, S. Gatson, M. Yokohari, R. Brown, Urban Climate **55**, 101888 (2024).
[134] Y. Kimura, T. Seki, K. Chujo, T. Murata, S. Miyata, H. Inoue, N. Ito, Scientific Reports **15**, 1081 (2025).
[135] M. Alidadi, A. Sharifi, D. Murakami, Sustainable Cities and Society **97**, 104743 (2023).
[136] S. Thapa, H. B. Rijal, S. A. Zaki, Sustainable Cities and Society **116**, 105840 (2024).
[137] Z. Li, D. Hu, Sustainable Cities and Society **78**, 103392 (2022).
[138] P. Zeng, F. Sun, Y. Liu, T. Tian, J. Wu, Q. Dong, S. Peng, Y. Che, Sustainable Cities and Society **78**, 103599 (2022).
[139] Y. Zhang, L. Chen, Y. Wang, L. Chen, F. Yao, P. Wu, B. Wang, Y. Li, T. Zhou, T. Zhang, Remote Sensing **7**, 10737 (2015).
[140] A. Guo, T. He, W. Yue, W. Xiao, J. Yang, M. Zhang, M. Li, International Journal of Applied Earth Observation and Geoinformation **125**, 103570 (2023).
[141] T. Cornu, B. Marchal, D. Renmans, BMC Public Health **24**, 457 (2024).
[142] E. K. Mohamed, A. M. El Kenawy, H. Aboelkhair, M. M. Abdelaal, I. Mohamed, B. Fernandez-Duque, D. Pena-Angulo, Sustainable Cities and Society **102**, 105236 (2024).
[143] P. K. Diem, C. T. Nguyen, N. K. Diem, N. T. H. Diep, P. T. B. Thao, T. G. Hong, T. N. Phan, Remote Sensing Applications: Society and Environment **33**, 101081 (2024).
[144] E. Lasky, S. Costello, A. Ndovu, R. Aguilera, S. D. Weiser, T. Benmarhnia, Science of the Total Environment **949**, 175284 (2024).
[145] M. Zoran, R. Savastru, D. Savastru, M. Tautan, Environmental Research **228**, 15907 (2023).
[146] J. Sola-Caraballo, A. Serrano-Jiménez, C. Rivera-Gomez, C. Galan, Marin, Remote Sensing **17**, 231 (2025).
[147] A. Esposito, G. Pappaccogli, A. Donateo, P. Salizzoni, G. Maffeis, T. Semeraro, J. L. Santiago, R. Buccolieri, Remote Sensing **16**, 4496 (2024).
[148] D. Melas, D. Parliari, T. Economou, C. Giannaros, N. Liora, S. Papadogiannaki, S. Kontos, S. Cheristanidis, D. Occhiuto, M. A. Frezzini, J. Kushta, T. Christoudias, C. Savvides, I. Christofides, G. Casasanta, S. Argentini, A. Progiou, G. Papastergiosm, A. Kelessis, Environmental Sciences Proceedings **26**, 117 (2023).
[149] Y. Zhang, Q. Sun, J. Liu, O. Petrosian, Sustainability **16**, 19 (2024).
[150] G. Xian, H. Shi, Q. Zhou, R. Auch, K. Gallo, Z. Wu, M. Kolian, Remote Sensing of Environment **269**, 112803 (2022).
[151] N. Yadav, K. Rajendra, A. Awasthi, C. Singh, B. Bhushan, Urban Climate **51**, 101622 (2023).
[152] I. Agathangelidis, C. Cartalis, M. Santamouris, Climate **8**, 131 (2020).
[153] J.-H. Kim, S.-J. Kim, J.-H. Kim, M. Hayashi, M. K. Kim, Scientific Reports **12**, 1 (2022).
[154] M. Wakayama, K. Mameno, T. Owake, T. Aikoh, Y. Shoji, Urban Forestry and Urban Greening **107**, 128771 (2025).
[155] M. Soga, K. J. Gaston, Nature Climate Change **14**(2), 108 (2024).
[156] F. Batibeniz, S. I. Seneviratne, S. Jha, A. Ribeiro, L. S. Gutierrez, C. C. Raible, A. Malhotra, B. Armstrong, M. L. Bell, E. Lavigne, A. Gasparrini, Y. Guo, M. Hashizume, P. Masselot, S. Pereira da Silva, D. Royé, F. Sera, S. Tong, A. Urban, A. M. Vicedo-Cabrera, Scientific Reports **15**, 1002 (2025).
[157] J. Ma, Y. Guo, J. Gao, H. Tang, K. Xu, Q. Liu, L. Xu, Biology **11**(11), 1628 (2022).
[158] L. Mentaschi, G. Duveiller, G. Zulian, C. Corbane, M. Pesaresi, J. Maes, A. Stocchino, L. Feyen, Global Environmental Change, **72**, 102441 (2022).

*Corresponding author: dsavas@inoe.ro